The measurement of electrostatic potentials in core/shell GaN nanowires using off-axis electron holography

Yazdi, Sadegh; Kasama, Takeshi; Ciechonski, R; Kryliouk, O; Wagner, Jakob Birkedal

Published in:
Journal of Physics - Conference Series

Link to article, DOI:
10.1088/1742-6596/471/1/012041

Publication date:
2013

Document Version
Publisher's PDF, also known as Version of record

The measurement of electrostatic potentials in core/shell GaN nanowires using off-axis electron holography

2013 J. Phys.: Conf. Ser. 471 012041

(http://iopscience.iop.org/1742-6596/471/1/012041)

The measurement of electrostatic potentials in core/shell GaN nanowires using off-axis electron holography

S Yazdi[1], T Kasama[1], R Ciechonski[2], O Kryliouk[3] and JB Wagner[1]

[1]Center for Electron Nanoscopy, Technical University of Denmark, Lyngby, Denmark

[2]GLO-AB, Ideon Science Park, Lund, Sweden

[3]GLO-USA, Sunnyvale, CA, United States of America

sadegh.yazdi@cen.dtu.dk

Abstract. Core-shell GaN nanowires are expected to be building blocks of future light emitting devices. Here we apply off-axis electron holography to map the electrostatic potential distributions in such nanowires. To access the cross-section of selected individual nanowires, focused ion beam (FIB) milling is used. Furthermore, to assess the influence of FIB damage, the dopant potential measured from an intact NW is compared with a FIB prepared one. It is shown that in addition to the built-in potential between the p-type shell and unintentionally n-type under-layer there is a potential barrier between the core and under-layer which are both unintentionally n-type doped.

1. Introduction

Light-emitting diodes (LEDs) are predicted to be able to reduce global electricity consumption for lighting by over 50% [1]. Since GaN-based material systems span the entire visible spectrum, GaN is becoming the material of choice in LEDs. Nanowires (NWs) are promising candidates for building blocks of GaN LEDs due to their defect-free crystal structure, large surface to volume ratio, and exposed non-polar *m*-plane, $\{1\bar{1}00\}$, along which the active region of devices can be grown [2]. However, the lack of ability to control the distribution of dopants along the nanowires has hindered the progress of nanowire-based devices [3]. Finding a precise doping process is very challenging in core-shell structured nanowires. For the development of new doping methods, comprehensive feedback is required from a dopant characterisation technique. Unfortunately the nano-scale geometry of nanowires hampers conventional characterisation techniques such as four point probes (4PP) and Hall-effect measurements. Here, we use off-axis electron holography in the transmission electron microscope (TEM) to measure the electrostatic potential built-in across the core/shell of GaN nanowires.

In the absence of dynamical diffraction and magnetic field, the phase shift that the electron beam experiences as it passes through a TEM specimen is expressed by:

$$\varphi(x,y) = C_E \int_0^t V(x,y,z)dz, \qquad \text{(Eq. 1)}$$

where C_E is a constant depending on the acceleration voltage of microscope, t is the specimen thickness and $V(x, y, z)$ represents the electrostatic potential distribution in the specimen. This phase shift can be measured by off-axis electron holography. If the specimen thickness and the potential distribution along the beam direction, z, are known, $V(x, y)$ can be extracted from the phase image.

2. Experimental details

The GaN NWs examined in this study were grown by catalyst-free metal organic chemical vapour deposition (MOCVD) on a sapphire substrate on which a GaN buffer layer was deposited. A schematic cross-section of the NW sample is shown in Fig. 1(a). The position of each nanowire was controlled using nano-imprint lithography [4]. Unintentionally n-type doped (hereafter referred to as "u-type") cores, shown in Fig. 1a, were nucleated and grown to a desirable length. Then, u-type under-layers (ULs) were grown around the core. By doping the shells with Mg (2.8% Mg/Ga ratio), pn junctions were formed between the u-type under-layers and p-type shells. A top-view scanning electron microscope (SEM) image of as-grown NWs is shown in Fig. 1(b). Two types of TEM specimen were prepared from the NWs using a dual beam (FIB/SEM) microscope equipped with a micromanipulator. The first type is a cross-sectional specimen prepared along the *a*-plane, $\{11\bar{2}0\}$, of the NWs using the *in-situ* lift-out technique and the second one is an intact single NW lifted up with the micromanipulator and placed on a TEM grid by electrostatic forces without using the FIB. Off-axis electron holograms were acquired at 300 kV in an FEI Titan 80-300 TEM, equipped with a rotatable Möllenstedt biprism.

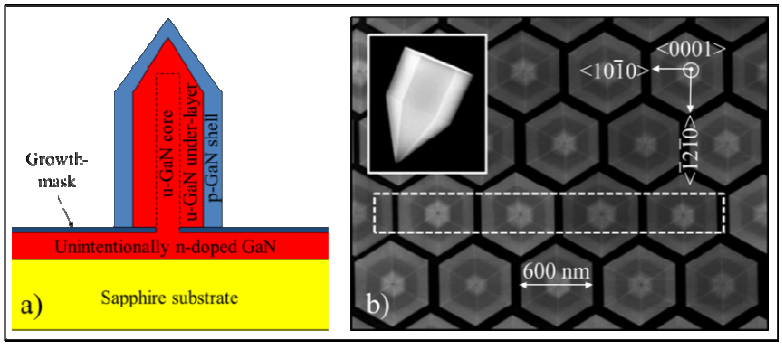

Fig. 1. a) Schematic showing the structure of nanowires used in this study. b) SEM micrographs acquired from as-grown nanowires along <0001> direction and <10$\bar{1}$0> direction (inset). The dashed box in this image shows the position from where the FIB specimen was prepared.

3. Results and discussion

3.1. FIB prepared specimen

A typical secondary electron image acquired with 2 keV electron beam from the cross-sectional surface of NWs after low voltage (2 kV) FIB polishing is shown in Fig. 2. The dopant contrast with higher secondary electron intensity on the p-type shell regions than on the u-type core and UL regions appeared only when the specimen surface was polished with less than 5 kV Ga ion beam. The dopant contrast in SEM was used as a criterion for minimising the FIB damage. Among available FIB voltages, from 30 kV down to 500 V in our dual beam microscope, 2 kV beam was chosen for the final specimen preparation step since the maximum dopant contrast was achieved after polishing the specimen surfaces with this beam voltage.

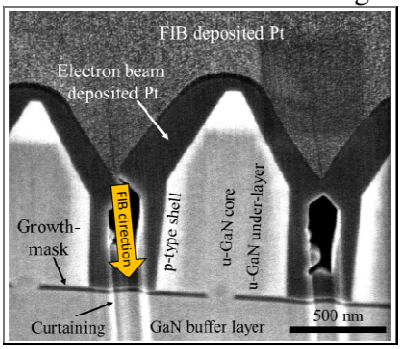

Fig. 2. A typical SEM image from a FIB prepared cross-sectional surface of NWs after 2kV FIB polishing. The SEM dopant contrast can be seen in this image. The FIB milling direction, shown by an arrow, was intentionally chosen not to be parallel to the NWs so that any possible thickness variations due to the curtaining effect would be distinguishable from electrostatic potential variations. It can be seen that the curtaining direction in the GaN buffer layer is different from the nanowire growth direction.

A reconstructed phase image from a FIB prepared cross-sectional NW is shown in Fig. 3(a). By tilting the specimen by ~5° away from the zone axis along the Kikuchi band center, the diffraction contrast was minimized while the UL-shell junction was kept edge-on. The crystalline thickness of the specimen was measured to be 300±10 nm using convergent electron beam diffraction. The measured crystalline thickness was in agreement, within the experimental error, with the thickness map obtained from the reconstructed amplitude image. The inelastic mean free path of 300 kV electrons in GaN was measured to be ~100 nm directly from a single GaN NW which has a known geometry and thickness. This value was used in calculating the thickness map from the amplitude image.

The entire 300 nm crystalline thickness was used to convert the reconstructed phase image into the potential map, without considering any "dead layer", a crystalline layer which is electrically damaged by FIB. The electrostatic potential profile across the NW, from the dashed box in Fig. 3(a), is shown in Fig. 3(b). The measured built-in potential across the UL-shell junction was only 0.3 V, significantly smaller than about 3V expected from the intended dopant concentrations used during the growth. Also surprisingly it was found that in addition to this potential barrier between the p-type shell and u-type UL, there is almost the same potential barrier between the u-type core and u-type UL. Further systematic studies are in progress to understand this additional potential barrier.

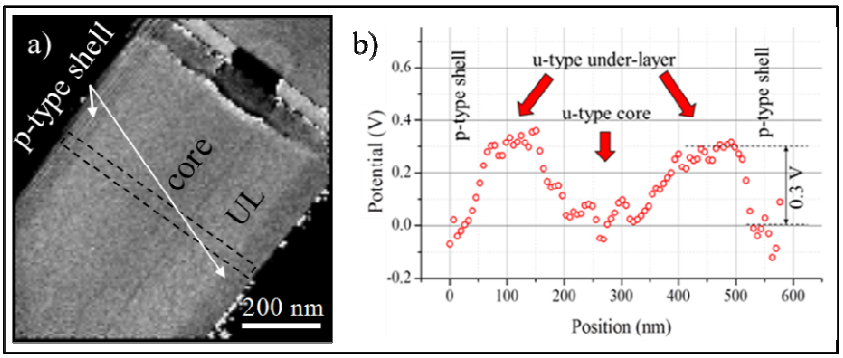

Fig. 3. a) Reconstructed phase image from a FIB prepared cross sectional NW. b) Potential profile from the region marked with the dashed box in (a).

3.2. Intact nanowire

To understand how significant the effect of FIB damage is on built-in potential measurements, electron holography on single intact NWs was carried out. As these NWs have a core-shell structure, the electrostatic potential variation along the electron beam direction needs to be taken into account in addition to the specimen thickness when converting the phase image into the potential map. For a core-shell NW, such as one shown in Fig. 4.a, Eq. 1 can be simplified as:

$$\varphi(x) = C_E V_{shell} t_{shell}(x) + C_E V_{core} t_{core}(x), \qquad \text{(Eq. 2)}$$

where V_{core} and V_{shell} refer to the electrostatic potential of the core and shell respectively. $t_{core}(x)$ and $t_{shell}(x)$ represent the core thickness and shell thickness at position x respectively. By calculating these thicknesses, using the geometry shown in Fig. 4(a), and substituting them into Eq. 2 the following expression is obtained for the phase shift of the electron beam:

$$\varphi(x) = C_E \begin{cases} (a + 2x\tan 30^o)V_{shell} \ ; & 0 \le x < \frac{\sqrt{3}}{2}(a-b) \\ 2(a-b)V_{shell} + (b + 2\left(x - (a-b)\frac{\sqrt{3}}{2}\right)\tan 30^o)V_{core} \ ; & (a-b)\frac{\sqrt{3}}{2} \le x < a\frac{\sqrt{3}}{2} \\ 2(a-b)V_{shell} + (b - 2\left(x - (a+b)\frac{\sqrt{3}}{2}\right)\tan 30^o)V_{core}; & a\frac{\sqrt{3}}{2} \le x < (a+b)\frac{\sqrt{3}}{2} \\ (a + 2(a\sqrt{3} - x)\tan 30^o)V_{shell} \ ; & (a+b)\frac{\sqrt{3}}{2} \le x < a\sqrt{3} \end{cases} \qquad \text{(Eq. 3)}$$

where a and b are the side lengths of the hexagonal shell and core respectively. According to Eq. 3, a phase step of $\Delta\varphi = C_E b V_{bi}$ close to the core-shell interface at $x = \frac{\sqrt{3}}{2}(a-b)$ and $x = \frac{\sqrt{3}}{2}(a+b)$ should be measurable.

The amplitude and phase images from an intact NW are shown in Fig. 4(b) and (c) respectively. By removing the phase slope, due to the thickness variation, in region B in Fig. 4(c), the phase step across the pn junction between the p-type shell and u-type UL appeared in the phase image, as can be seen in Fig 4(f). The potential profile in Fig. 4(g) is obtained by dividing the phase profile from the dashed box in Fig. 4(f) by $C_E b$ ($V_{bi} = \Delta\varphi/C_E b$). The measured built-in potential across the shell-UL junction is only 0.4 V. This means that in our FIB prepared cross-sectional specimen the effect of FIB damage on the potential measurements is not severe. Therefore, the smallness of the measured built-in potential cannot be explained solely by FIB damage. Other possible sources of error in electron holography measurements such as charging and electron-hole pair generation as a result of electron irradiation also need to be assessed. It is also likely that in these NWs the dopant atoms have not been distributed properly during the growth or they have not been activated completely. Work is in progress to investigate these possibilities.

The built-in potential close to the tip of the NW in region A (Fig. 4(c)) was measured to be 0.55 V. The flattened phase image in this region, obtained by removing the thickness variation, and its corresponding potential profile are shown in Fig. 4(d) and (e) respectively. Since this potential is along the *c*-axis, it is speculated that the internal polarisation field affects the value of this potential.

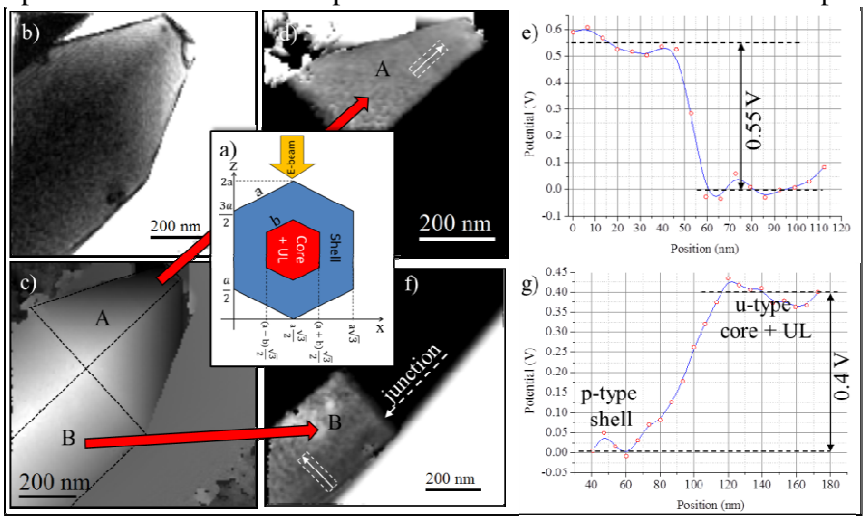

Fig. 4. a) The NW geometry and its orientation relative to the electron beam. b) Reconstructed amplitude and c) phase image from an intact NW. The phase image after removing the phase slope d) in A region and f) in B region. These regions are marked in (c). e) and g) show the potential profiles from the regions marked with dashed white boxes in (d) and (f) respectively.

4. Conclusion

Off-axis electron holography has been applied to a FIB prepared cross sectional GaN NW specimen for measuring electrostatic potential distributions. The built-in potential across the UL-shell junction was found to be 0.3 V in a FIB prepared specimen and 0.4 V in an intact NW. Therefore FIB damage cannot be solely responsible for the smallness of measured potentials. It was also found that there is a potential barrier between the core and UL. Further studies are in progress to expand our understanding of potential distributions in GaN NWs. This can lead us to fabricate more efficient GaN based LEDs.

References

[1] Tsao JY 2004 *Circuits and Devices Magazine IEEE* **20** 28
[2] Storm K *et al.* 2012 *Nature Nanotechnology* **7** 718
[3] Wallentin J *et al.* 2011 *J. Mater. Res.* **26** 2142
[4] Mårtensson T *et al.* 2004 *Nano Lett.* **4** 699
[5] The authors acknowledge funding from 'Nanowires for solid state lighting'. NMP.2011.2.2-3, Project ID:280773